# NONLINEAR 3D MAGNETOSTATIC FIELD CALCULATION BY THE INTEGRAL EQUATION METHOD WITH SURFACE AND VOLUME MAGNETIC CHARGES

by B. Krstajić, Z. Anđelić, S. Milojković and S. Babić

Elektrotehnički fakultet Sarajevo
71000 Sarajevo
Yugoslavia

S. Salon

Electrical Power Engineering
Rensselaer Polytechnic
Troy, New York 12180-3590

**Abstract:** This paper presents a mathematical model for the 3D nonlinear magnetostatic field based on integral equations with fictitious surface and volume magnetic charges. The solution is performed by the Extended Boundary Element Method including Surface Elements (SE) and Volume Elements (VE). Examples of the calculation for both linear and nonlinear magnetic systems are presented.

## Introduction

The mathematical models for the 3D fields can be divided into three categories: 1) differential, in which the unknown functions are expressed in terms of partial differential equations with specified boundary conditions, 2) integral equations, in which the boundary conditions are implied and, 3) hybrid methods, in which different subdomains of the problem are represented by differential or integral equations. While integral equations, and in particular the boundary element method, has many advantages over differential methods, a major drawback is the difficulty in dealing with nonlinear materials. The present method uses the extended boundary element method with surface and volume elements in which the unknowns are equivalent surface and volume magnetic charges.

## Mathematical model

Consider the problem of Fig. 1, in which we have both current carrying conductors and nonlinear ferromagnetic material having a magnetization characteristic $B=\mu(H)H$.

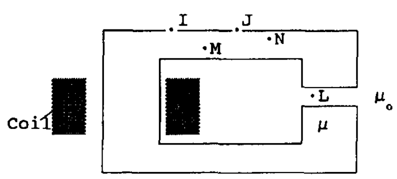


Fig. 1 *Electromagnet model*

We introduce an equivalent normalized surface magnetic charge density

$$\sigma(s)=\frac{\sigma_m(s)}{\mu_0}$$

on the boundary surface and an equivalent normalized magnetic charge density

$$\rho(v)=\frac{\rho_m(v)}{\mu_0}$$

distributed in the volume of the magnetic material.

Manuscript received July 7, 1991; revised September 17, 1991.

Thus the magnetic field can be found as the sum of two components

$$\vec{H}=\vec{H}^J+\vec{H}^M \tag{1}$$

where $\vec{H}^J$ is the component of field which would be produced by the steady currents in free space and $\vec{H}^M$ is the component produced by the magnetic charges.

For point $I$ lying on the boundary

$$B_n^i(I)=B_n^o(I), \qquad \mu(I)H_n^i(I)=\mu_o H_n^o(I).$$

From these boundary conditions we find the following integral equation:

$$\sigma(I)-\frac{\lambda(I)}{2\pi}\iint_{S_J}\sigma(J)\cdot\frac{(\vec{r}_{IJ},\vec{n}_i^o)}{r_{IJ}^3}dS_J=2\lambda(I)H_n^J(I)+\frac{\lambda(I)}{2\pi}\iiint_{V_N}\rho(N)\cdot\frac{(\vec{r}_{IN},\vec{n}_i^o)}{r_{IN}^3}dV_N \tag{2}$$

where $\qquad \lambda(I)=\dfrac{\mu_r(I)-1}{\mu_r(I)+1}.$

Using the fact that inside the magnetic material we have:

$$\nabla\cdot\vec{B}(M)=0, \qquad \nabla\cdot\vec{H}^J(M)=0, \qquad \vec{H}^M(M)=-\nabla\varphi_m^M(M)$$

($\varphi_m^M$ - reduced scalar potential)

we can write

$$\rho(M)=-\nabla(\ln\mu_r(M))\cdot\vec{H}(M). \tag{3}$$

To use equation (3) we must compute the field inside the magnetic material. Equation (1) gives large errors inside magnetic material, so we use a corrected value of surface charge $\sigma_t(s)$ which accounts for the demagnetization effects. The magnetic field vector at point $M$ inside the material is found as:

$$\vec{H}(M)=\frac{1}{4\pi}\iint_{S_J}\sigma_t(J)\cdot\frac{\vec{r}_{MJ}}{r_{MJ}^3}dS_J+\frac{1}{4\pi}\iiint_{V_N}\rho(N)\cdot\frac{\vec{r}_{MN}}{r_{MN}^3}dV_N \tag{4}$$

The relative permeability is

$$\mu_r=\frac{B(H(M))}{\mu_o H(M)} \tag{5}$$

For points in the air or points on the magnetic surface

$$\vec{H}(I)=\frac{1}{4\pi}\iint_{S_J}\sigma(J)\cdot\frac{\vec{r}_{MJ}}{r_{MJ}^3}dS_J+\frac{1}{4\pi}\iiint_{V_N}\rho(N)\cdot\frac{\vec{r}_{MN}}{r_{MN}^3}dV_N+\vec{H}^J(I) \tag{6}$$

0018-9464/92$03.00 

For a given set of steady currents it is possible to calculate the magnetic field $\vec{H}'$, [1] and [2]. So, with a known magnetization characteristic $B=B(H)$, equations (1)-(6) give a complete mathematical model of the nonlinear 3D magnetostatic field, based on normalized surface and volume charges.

## Numerical procedure

To solve (1)-(6) we use the Extended Boundary Element Method. The extended method uses surface elements (SE) and volume elements (VE). The surface elements are the approximated parts of the boundary surfaces [3], and the volume elements are the approximated parts of the volume that lays inside of the boundary surface. As elements there are also used the analytically described parts of the boundary surface [4] and volume, i.e. partial SE and VE.

In the Extended Boundary Element Method the unknowns become a set of functions described on the elements. To describe these unknown functions we use a set of basis functions. If there are known the function values in the $m$ appropriately selected points of the element, than the function value in the arbitrary point of the element can be calculated as:

$$f=\sum_{j=1}^{m} N_j \cdot f_j=[N^{(e)}][f^{(e)}]. \tag{7}$$

For the unknown function $\rho^{(v)}$ in the VE we use a constant value assigned to the center of the element. For the functions $\sigma^{(s)}$ and $\sigma_f^{(s)}$ on the SE and for $\vec{H}^{(v)}$ and $\mu_r^{(v)}$ in the VE we use linear basis functions. For the geometry of elements we use a quadratic approximation, or they are presented by the partial elements. With this representation the 3D nonlinear magnetostatic field can be written as a set of algebraic equations as follows:

$$[\sigma]-[\lambda][A][\sigma]=[\lambda]\{[D][\rho]+[B]\} \tag{8}$$

where an element of $[\rho]$ is:

$$\rho^{(v)}(T)=-\nabla(\ln\{[N^{(1)}(T)][\mu_r^{(v)}]\})\cdot\{[N^{(1)}(T)][\vec{H}^{(v)}]\} \tag{9}$$

and an element of $[\vec{H}^{(v)}]$ and $[\mu_r^{(v)}]$ are found as:

$$\vec{H}^{(v)}=[\vec{A}_1][\sigma_f]+[\vec{D}_1][\rho]$$

and $$\mu_r=\frac{B(H^{(v)})}{\mu_o H^{(v)}} \tag{10}$$

Since the SE nodes are a subset of the VE nodes, $\mu_f^{(I)}$ can be found from (10). In the linear case $[\lambda]$ is constant and $[\rho]=[0]$. For nonlinear problems (8)-(10) are solved iteratively using the linear case as a starting point. The equations converge rapidly and stably.

## Examples

In order to verify the present method, especially to confirm the applicability of the mathematical model and numerical procedure, four examples of linear and nonlinear problems are presented. The results are compared with alternate calculation methods.

**Example 1.** *A spherical linear magnetic medium in a uniform magnetic field*

A spherical magnetic medium, $R=0{,}1$ m and $\mu=998$, is situated in homogeneous magnetic field $H_o=50$ A/m. An exact solution of the problem is given for

- the points inside the sphere:

$$\vec{H}=\frac{3}{\mu_r+2}H_o\vec{k} \tag{11}$$

- the points outside the sphere in the plane $y=0$:

$$H_x(x,0,z)=\frac{\mu_r-1}{\mu_r+2}\cdot\frac{3R^3xzH_o}{(x^2+z^2)^{5/2}} \tag{12}$$

$$H_z(x,0,z)=H_o+\frac{\mu_r-1}{\mu_r+2}\cdot\frac{3R^3z^2H_o}{(x^2+z^2)^{5/2}}-\frac{\mu_r-1}{\mu_r+2}\cdot\frac{R^3H_o}{(x^2+z^2)^{3/2}} \tag{13}$$

Due to the symmetry only 1/8 part of the sphere is considered. The mesh consists of 71 triangle SE and 51 nodes. The boundary surface discretization is presented on the Fig. 2.

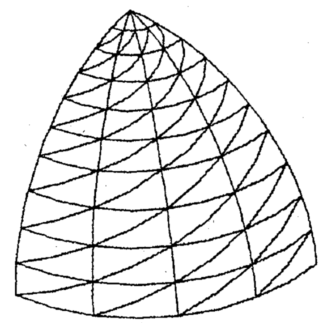

Fig. 2 *The discretization of 1/8 sphere*

Both, the analytical and numerical calculation results are presented in Table 1. The calculation error is less then 0.8%. For the comparison the calculation error in [6] is up to 3% for approximatly same number of surface elements.

Table 1.

| $y=0$ | | Analytical | | Numerical | |
|---|---|---|---|---|---|
| $x(m)$ | $z(m)$ | $H_x(A/m)$ | $H_z(A/m)$ | $H_x(A/m)$ | $H_z(A/m)$ |
| 0.00 | 0.00 | 0.000 | 0.150 | 0.000 | 0.151 |
| 0.05 | 0.00 | 0.000 | 0.150 | 0.000 | 0.151 |
| 0.1- | 0.00 | 0.000 | 0.150 | 0.000 | 0.151 |
| 0.1+ | 0.00 | 0.000 | 0.150 | 0.000 | 0.151 |
| 0.15 | 0.00 | 0.000 | 35.230 | 0.000 | 35.142 |
| 0.00 | 0.05 | 0.000 | 0.150 | 0.000 | 0.151 |
| 0.05 | 0.05 | 0.000 | 0.150 | 0.000 | 0.151 |
| 0.10 | 0.05 | 42.804 | 35.732 | 43.116 | 35.707 |
| 0.00 | 0.1+ | 0.000 | 149.70 | 0.005 | 149.698 |
| 0.00 | 0.1- | 0.000 | 0.115 | 0.000 | 0.115 |
| 0.05 | 0.10 | 42.804 | 99.938 | 42.825 | 100.152 |
| 0.00 | 0.15 | 0.000 | 79.541 | 0.000 | 79.616 |

**Example 2.** *Two spherical linear magnetic substances in a uniform magnetic field*

Fig. 3 presents the arrangement consisting of two spherical linear media in the homogeneous magnetic field.

Due to the symmetry it is observed only 1/4 of the system with 608 elements and 346 nodes. Fig. 4 and 5 present the distribution of field component $H_z$, calculated in the points along the line 1 and 2, respectively.

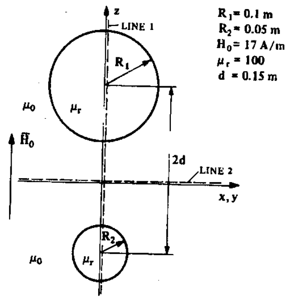


Fig. 3 *The arrangement of two iron spheres*

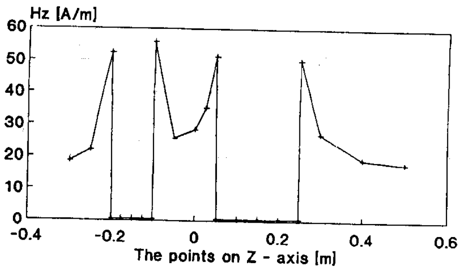


Fig. 4 *Example 2: The $H_z$ component along the line 1. ("+" - 2D results)*

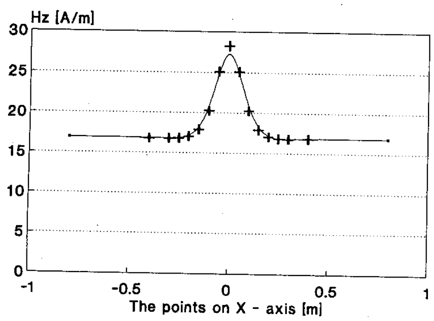


Fig. 5 *Example 2: The $H_z$ component along the line 2. ("+" - 2D results)*

**Example 3.** *Standard problem proposed by IEEJ*

The method has also been applied to the standard problem proposed by The Institute of Electrical Engineers of Japan, [5], [6]. Fig. 6 displays this standard problem. The permeability of the iron core is 1000 and magnetomotive force 3000 AT.

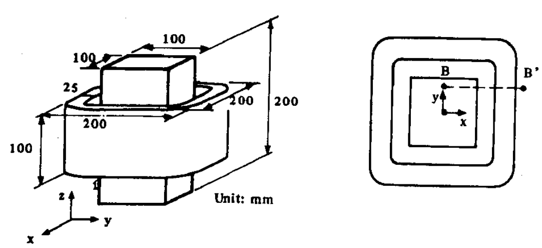


Fig. 6 *Standard problem proposed by IEEJ*

Only 1/8 of the problem is considered, having more dense discretization close the edges, Fig. 7, with 738 SE and 404 nodes. Fig. 8 displays $z$ component distribution of the magnetic flux density along the $x$ coordinate 10 mm away from the top surface of the iron core, along the line with $y$=45 mm. The diference between calculation and experimental results is less then those presented in [6].

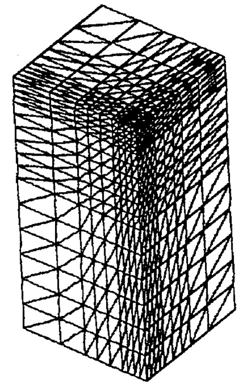

Fig. 7 *Example 3: Surface element structure*

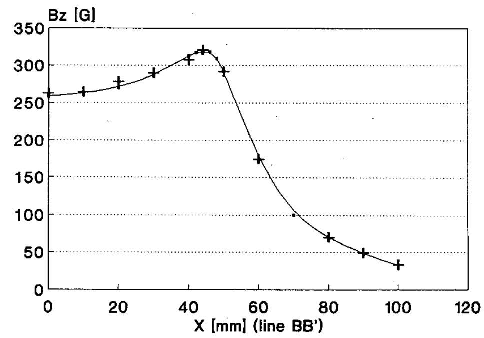


Fig. 8 *Example 3: $B_z$ over the top surface, line B-B' ("+" - experiment)*

**Example 4.** *Iron cylinder in the field of a cylindrical coil* [7]

This example presents the calculation of 3D nonlinear magnetic field by the method described in this paper. An iron cylinder in the field of a cylindrical coil is considered, Fig. 9.

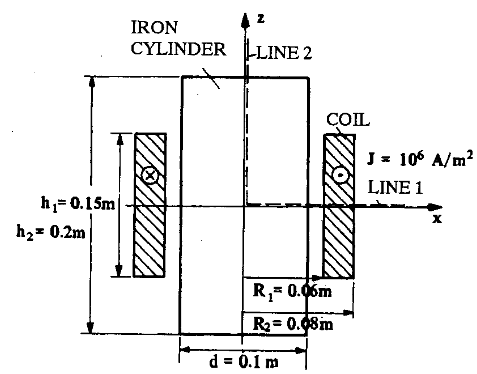


Fig. 9 *Iron cylinder in the field of a cylindrical coil*

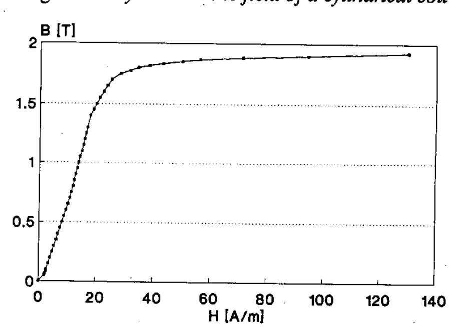


Fig. 10 *Example 4: The B-H curve*

The medium characteristic is given over $B=B(H)$ magnetization curve, Fig. 10. Due the symmetry, only one 1/8 of the system is taken into consideration, Fig. 11, having 235 SE and 715 VE. The number of the SE nodes is 145 and the number of the VE nodes is 938. It was chosen $\mu_r=55000$ for the start value of the iterative calculation.

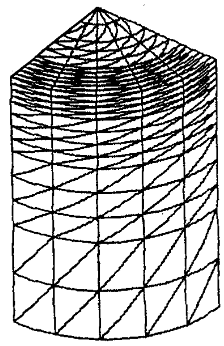

Fig. 11 *Example 4: SE structure*

The direct iteration was stopped when the mean alteration of the material became sufficiently small. This alteration was calculated as:

$$a_m^{(i)}=0.5\Big(\frac{1}{NV}\sum_M a^{(i)}(M)+\max_M(a^{(i)}(M)\Big)=0.5(a^{(i)}_{mean}+a^{(i)}_{max,local}) \quad (14)$$

$NV$ - number of the VE nodes, and

$$a^{(i)}(M)=\frac{|\mu_r^{(i)}(M)-\mu_r^{(i-1)}(M)|}{\mu_r^{(i)}(M)} \quad (15)$$

Fig. 12 shows the alteration during the iterative procedure. The convergence of the procedure does not depend on the start value $\mu_r$.

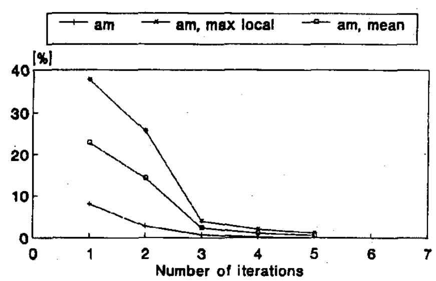


Fig. 12 *Example 4: The alteration during the iterative calculation*

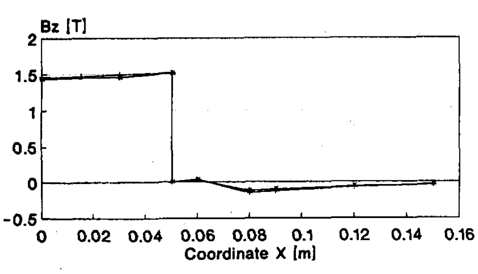


Fig. 13 *Example 4: The $B_z$ component along the line 1. ("+" - ref. [7])*

The calculation results for the $B_z$ component along the lines 1. and 2. are presented on Fig. 13 and 14, respectively. These results coincide with those given in [7] for the same example.

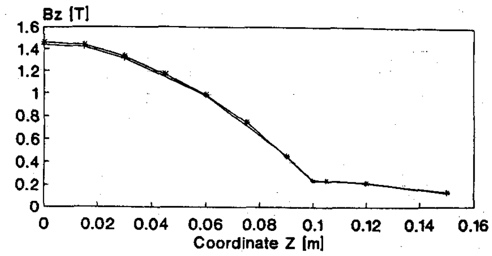


Fig. 14 Example 4: *The $B_z$ component along the line 2. ("+" - ref. [7])*

## Conclusions

The linear and nonlinear 3D magnetostatic problems have been solved using the extended boundary element method. The method has been shown to be accurate and efficient.

## Acknowledgement

This research is supported by the US National Science Foundation under contact #JF 824.

## References

[1] S. Babić, B. Krstajić, S. Milojković and Z. Andjelić, "An Efficient Approach for the Calculation of 3D Magnetostatic Field of Current-Carrying Regions of Typical Form", IEEE Trans. on Mag., Vol. MAG-24, No. 1, January 1988, pp. 423-426.

[2] S. Babić, Z. Andjelić, B. Krstajić and S. Salon, "Analytical Calculation of the 3D Magnetostatic Field of a Torroidal Conductor with Rectangular Cross Section", IEEE Trans. on Mag., Vol MAG-24, No. 6, November 1988, pp. 3162-3164.

[3] Z. Andjelić, B. Krstajić and S. Milojković, "A Procedure for Automatic Optimal Shape Investigation of Interfaces between Media", IEEE Trans. on Mag., Vol. MAG-24, No. 1, January 1988, pp. 415-418.

[4] B. Krstajić, Z. Andjelić and S. Milojković, "An Improvement in 3D Electrostatic Field Calculation", Fifth Int. Symp. on High Voltage Engineering, Brunschweig FGR, 1987, paper 31-02.

[5] M. Koizumi, M. Onisawa and M. Utamura, "Three-Dimensional Magnetic Field Analysis Method Using Scalar Potential Formulated by Boundary Element Method", IEEE Trans. on Mag., Vol. 26., No. 2, March 1990., pp. 360-363.

[6] K. Sawa and T. Hirano, "An Evaluation of the Computational Error near the Boundary with Magnetostatic Field Calculation by B.E.M", IEEE Trans. on Mag., Vol. 26., No 2., March 1990., pp. 403-406.

[7] Ch. Magele, H. Stogner and K. Preis, "Comparison of Different Finite Element Formulations for 3D Magnetostatic Problems" IEEE Trans. on Mag., Vol. 24., No 1., January 1988., pp. 31-34.